

LETTER TO THE EDITOR

Magnetic polaron conduction above the Curie temperature in Fe-doped $\text{Pr}_{0.75}\text{Sr}_{0.25}\text{MnO}_3$

J-M Liu^{1,2,4}, T Yu³, Q Huang^{1,3}, J Li^{1,3}, Z X Shen³ and C K Ong^{1,3}

¹ Laboratory of Solid State Microstructures, Nanjing University, Nanjing 210093, People's Republic of China

² Laboratory of Laser Technologies, Huazhong University of Science and Technology, Wuhan 430074, People's Republic of China

³ Department of Physics, National University of Singapore, 119260, Singapore

⁴ International Centre for Materials Sciences, Chinese Academy of Sciences, Shenyang 110016, People's Republic of China

E-mail: liujm@nju.edu.cn

Received 23 January 2002

Published 1 February 2002

Online at stacks.iop.org/JPhysCM/14/L141

Abstract

The transport behaviour of Fe-doped $\text{Pr}_{0.75}\text{Sr}_{0.25}\text{MnO}_3$ (PSMFO, Fe = 0.05) is studied by zero-field conductivity probing and Raman spectroscopy. It is revealed that the conductivity of PSMFO above T_m , the metal–insulator transition point, shows variable-range-hopping behaviour instead of the small-polaron mode. The B_{2g} Raman line at 630 cm^{-1} arising from the Mn–O bending and stretching modes undergoes anomalous softening as the temperature is lowered from ambient temperature, indicating a magnetic ordering sequence above T_m . It is demonstrated that the electronic conduction of PSMFO above T_m is governed by magnetic polarons embedded in a matrix of paramagnetic insulating phase.

(Some figures in this article are in colour only in the electronic version)

Colossal-magnetoresistance (CMR) perovskite manganites with the chemical formula $\text{R}_{1-x}\text{A}_x\text{MnO}_3$, where R is a rare-earth metal and A is an alkaline earth: Sr, Ca, Ba, Pb, have been receiving attention recently, as they display a range of transport and magnetic properties consistent with a strongly correlated electron system [1]. The electronic transport of the system experiences an insulator–metal transition as temperature T decreases, with the resistivity around the transition point T_m being significantly influenced by the external magnetic field H , resulting in the so-called CMR effect [1]. This effect can be understood in the framework of the double-exchange (DE) model proposed by Zener [2], but the coupling between the carriers and the phonon system through a Jahn–Teller distortion must be included in order to take into account the conductivity in the insulating phase above T_m [3].

However, the published data on the conduction mechanism above T_m are somewhat controversial [3–5]. Initially, the small-polaron concept was proposed to explain this type of

coupling, while the variable-range-hopping mode was also employed to fit the data on various manganites, as is frequently done for amorphous semiconductors [6]. Other measurements suggested that some manganites are inhomogeneous, with coexistence of spin-ordered and disordered regions [7–9]. Furthermore, the small-polaron mechanism may no longer work and the magnetic polaron was proposed on the basis of spin-polarized neutron scattering (large and small angle) [7, 9, 10], and Mössbauer [11] and transport measurements, although some inconsistent data were reported at the same time [10]. The magnetic polaron mechanism has been evidenced with data for $\text{La}_{1-x}\text{Ca}_x\text{MnO}_3$ and $\text{La}_{1-x}\text{Sr}_x\text{MnO}_3$ ($x = 0.1\text{--}0.5$), for example. A simple picture has the microstructure above T_m consisting of magnetic polarons (small spin clusters) embedded in a paramagnetic matrix [11]. On one hand, the magnetic polarons which display a superparamagnetic relaxation grow and coalesce, and a ferromagnetic transition occurs as T is lowered through T_m ; on the other hand, similar cluster growth and coalescence are observed above T_m upon application of H . The concept of the magnetic polaron has thus become physically acceptable, because minimal lattice distortion above T_m was confirmed in a range of systems with reasonable divalent substitution of the rare-earth metal component.

A direct argument associated with the magnetic polaron concept states that the magnetic polarons should be favoured in typical inhomogeneous manganites with minimal distortion. One case is that of Fe-doped manganites. Fe^{3+} and Mn^{3+} have similar ion radii and show similar 4d electrons in the outer shell. Upon Fe doping, little lattice distortion is expected. Fe ions substitute at Mn-ion sites, while this doping presents an antiferromagnetic background, therefore favouring insulating conduction and slightly disfavours DE ferromagnetism [12]. Because of the Fe doping, the Mn–O–Mn network and Fe–O–Mn network coexist, thus enhancing the system's magnetic inhomogeneity. In this letter, we study the conductivity and magnetic ordering of $\text{Pr}_{1-x}\text{Sr}_x\text{MnO}_3$ above T_m , with and without Fe doping, in order to demonstrate the inhomogeneity-induced effect. Although the transport and CMR behaviours of some Fe-doped $\text{La}_{1-x}\text{A}_x\text{MnO}_3$ single crystals and ceramics have been investigated [12, 13], the present work focuses on Pr-based manganites with Fe-doping-induced inhomogeneity. We study two samples: $\text{Pr}_{0.75}\text{Sr}_{0.25}\text{MnO}_3$ (PSMO) and $\text{Pr}_{0.75}\text{Sr}_{0.25}\text{Mn}_{0.95}\text{Fe}_{0.05}\text{O}_3$ (PSMFO), noting that substitution of Sr for Pr at $x = 0.25$ certainly results in quasi-cubic structure with the minimal lattice distortion (the average A-site ionic radius is only 0.133, so the cooperative distortion of Mn–O octahedra is very small) [14]. A Mn-site substitution of 5% Fe does not enhance the distortion at all. Presenting the temperature-dependent resistivity and magnetization data and using Raman spectroscopy, we demonstrate the existence of magnetic polarons in this system above T_m .

The PSMO and PSMFO ceramic samples were prepared by conventional sintering processing. The samples are dense, with the density very close to the ideal value. The grain size is 80–100 nm diameter. Fine-step θ – 2θ x-ray diffraction (XRD) was used to characterize the single-phase crystallinity of the samples. The standard four-probe method was employed to measure the sample resistivity under zero field and $H = 3.0$ kOe applied along the current direction, over a temperature range 78–325 K. The temperature-dependent magnetization M was probed by an Oxford superconducting vibrating spectrometer (VSM). In this study, we are mainly concerned with the magnetic ordering effects above T_m . Because Raman scattering is sensitive to the lattice vibrations and the magnetic ordering effects [15, 16], we utilize Raman spectroscopy to probe the dependence of the lattice vibrations in this system on temperature. For the Raman experiment, the samples were put into a closed-cycle refrigerator (TMS 93 Linkam stage) capable of keeping the temperature as much as 100 K below the ambient temperature. The measurement was performed on the sample surface using the backscattering configuration. The laser source is an argon-ion laser with wavelength 488 nm together with a He–Ne laser of wavelength of 632.8 nm. The spectrometer is an ISA Jobin-Yvon-Spex T64000 Triple system with a liquid-nitrogen-cooled CCD detector. The accuracy of the temperature control is ± 0.1 K.

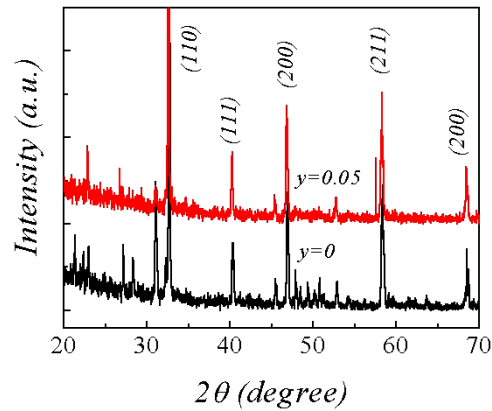


Figure 1. XRD θ - 2θ diffraction spectra for PSMO and PSMFO samples.

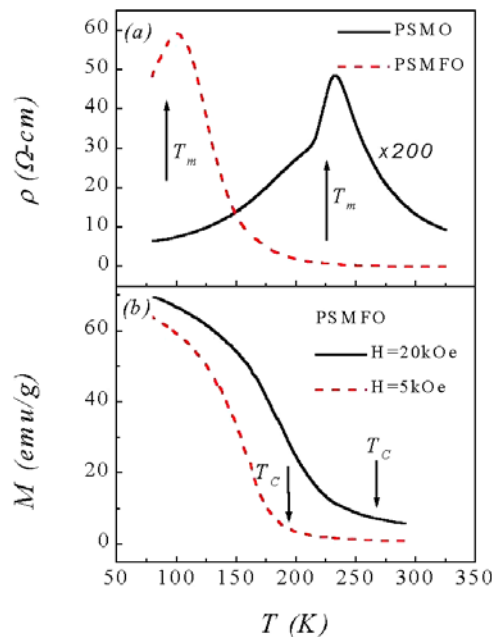


Figure 2. (a) Zero-field resistivity curves for PSMO and PSMFO samples and (b) the magnetization curves for PSMFO under two different fields. T_m for the metal-insulator transition and T_c for the ferromagnetic transition.

Figure 1 presents the XRD spectra of PSMO and PSMFO samples at ambient temperature. The samples are single phased and well crystallized. Like $\text{La}_{0.75}\text{Sr}_{0.25}\text{MnO}_3$, PSMO is rhombohedral (space group $R\bar{3}c$) as evidenced by the data shown in figure 1. We detect no structural change due to the Fe doping from the diffraction spectra. In fact, it has already been indicated that no structural change can be detected unless the doping is over 12% [14].

The zero-field resistivity ρ_0 as a function of T is presented in figure 2(a) for the two samples; we also show the magnetization $M(T)$ for PSMFO under two different fields, in figure 2(b). Well-defined temperatures $T_m = 225$ K for PSMO and $T_m = 95$ K for PSMFO are

observed, whereas ρ at the peak for PSMFO is two orders of magnitude higher than that for PSMO. The tremendous influence of the Fe doping on the transport properties is characterized by the remarkable shift of T_m toward the low- T side and the seriously damaged conductivity over the low- T range. In the meantime, one observes a typical ferromagnetic transition for each of the two samples as T is lowered. The transition point T_c as defined by the Curie–Weiss law is much lower for PSMFO ($T_c = 190$ K at $H = 5$ kOe) than for PSMO ($T_c = 250$ K). These findings are understandable considering the fact that Fe doping favours insulating behaviour and presents an antiferromagnetic background. Here, the interesting point is that for the PSMFO sample the observed T_c is much higher than T_m , with a difference over 100 K. Such an effect is inconsistent with the well-established prediction that the two transitions should occur simultaneously [1]. Furthermore, the measured T_c is sensitive to the applied field in the VSM, as displayed in figure 2(b), where T_c under $H = 20$ kOe is ~ 70 K higher than T_c under $H = 5$ kOe. These data predict the existence of small magnetic clusters when the PSMFO sample is still in the insulating phase ($T > T_m$), resulting in remarkable field dependence of the magnetization above T_m . These clusters will grow and coalesce as either T is lowered or H is applied.

Given the argument that PSMFO contains small magnetic clusters embedded in the paramagnetic and insulating matrix when $T > T_m$, one may propose a variable-range-hopping (VRH) conduction [6]:

$$\rho = \rho_{i0} \exp(T_0/T)^{1/4} \quad (1)$$

where ρ_{i0} is the prefactor and T_0 is the characteristic temperature. Otherwise, the small-polaron mode should be operative and the resistivity above T_m should follow [1]

$$\rho = \rho_{j0} T \exp(-E_0/kT) \quad (2)$$

where ρ_{j0} is the prefactor, E_0 is the activation energy for small polarons and k is the Boltzmann constant.

Plots of $\rho(T)$ data for PSMO and PSMFO samples according to equations (1) and (2) are presented in figures 3(a) and (b), respectively. For PSMO, the data agree well with the prediction of both VRH and small-polaron mechanisms, making an identification of the conduction mechanism impossible only from the transport behaviour. However, the conduction of PSMFO simply follows the VRH mode rather than the small-polaron mechanism, as identified in figure 3(b). Apart from the data around T_m , a good linear $\ln \rho \sim T^{-1/4}$ relationship (VRH) is observed, whereas no satisfactory linear $\ln(\rho/T) \sim T^{-1}$ behaviour (small-polaron behaviour) is identified. This indicates that the conduction of PSMFO above T_m is not dominated by small polarons, although the VRH conduction alone does not indicate dominance of the magnetic polaron conduction.

More evidence on the existence of magnetic polarons in PSMFO above T_m is supplied by our Raman scattering experiments. As an example, we present in figure 4 the measured Raman shift at various temperatures for PSMO (figure 4(a)) and PSMFO (figure 4(b)), respectively. The measurement was for no specific configuration and the laser beam was unpolarized since the samples are polycrystalline. Some Raman phonon modes may not be active in the present samples. What should be noted here is that our samples are very close to cubic alignment in the lattice and little contribution from the Jahn–Teller distortion to the scattering spectrum is observable. Therefore, the observed Raman-shift line should be broad and weak. We observed only two anomalous broad lines roughly at the positions ~ 430 and ~ 640 cm^{-1} . The former remains unassigned, as indicated previously, while the latter is actually a doublet of two broad lines near 630 cm^{-1} (B_{2g}) and 670 cm^{-1} [15, 16]. The lines at ~ 430 cm^{-1} are too weak to be analysed accurately for both samples unless T is very low. We thus focus on the evolution of the ~ 640 cm^{-1} line with temperature. In our samples, the contribution from the 670 cm^{-1}

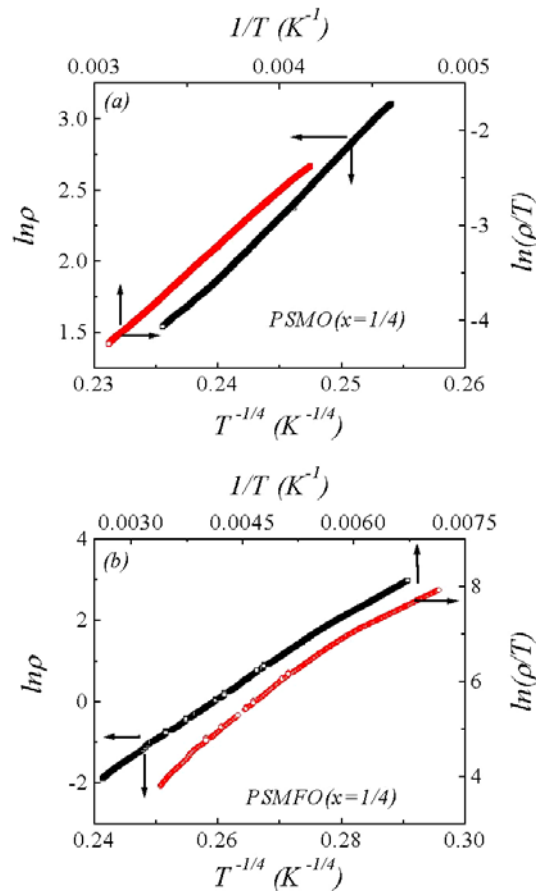


Figure 3. Fitting of the zero-field resistivity using a VRH model and a small-polaron model for (a) PSMO and (b) PSMFO samples. The unit for ρ is Ω cm and for T it is K.

line is quite weak because the observed line composed of those at ~ 630 and 670 cm^{-1} is at ~ 640 cm^{-1} , very close to ~ 630 cm^{-1} . In fact, by fitting with a sum of Lorentzians, one sees that the line at ~ 670 cm^{-1} is very weak. Thus, the measured 640 cm^{-1} linewidth remains largely temperature independent. A detailed discussion on this dependence was given earlier [15].

The 630 cm^{-1} line is usually related to the density of vibrational states, in particular the Mn–O bending and stretching modes [15]. The appearance of magnetic clusters in the structure and their evolution are characterized by the anomalous softening of these modes, because of a spin-correlation effect in the inter-ionic interaction, reflected by the Raman-line shift toward the low value. This softening effect exists independently of whether the metal–insulator transition appears or not [15]. Nevertheless, one finds from figure 4(a) that for PSMO there is no identifiable line shift within our experimental uncertainties when $T > 230$ K, close to $T_m \sim 220$ K and $T_c \sim 250$ K. The line intensity remains relatively low too. When $T < 230$ K, the line begins to shift toward the low-value side and the line intensity increases significantly, indicating the softening of the Mn–O bending and stretching modes. The line position evaluated as a function of T is presented in figure 5. This result is consistent with the observation for $\text{La}_{1-x}\text{Ca}_x\text{MnO}_3$ [15]. However, for the PSMFO sample, the line shift has

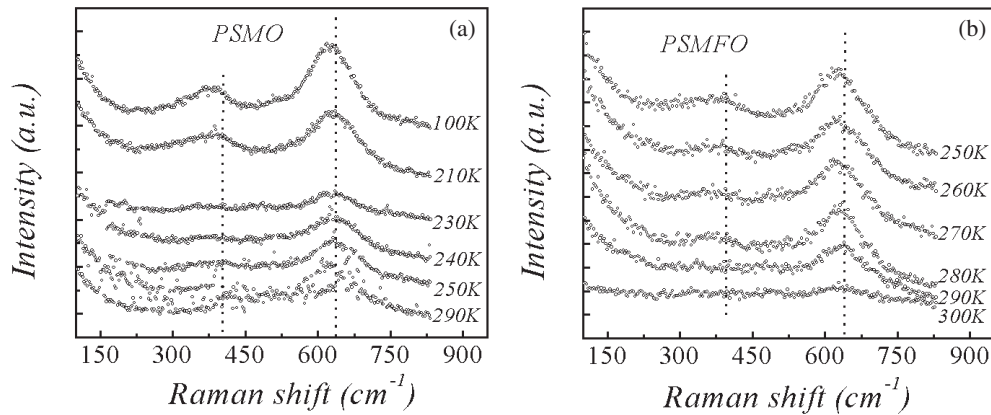


Figure 4. Raman scattering spectra for (a) PSMO and (b) PSMFO samples at different temperatures as indicated.

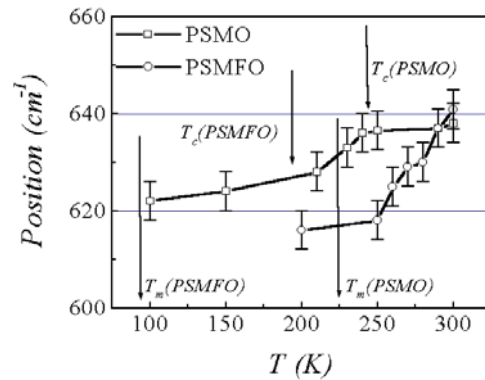


Figure 5. Temperature dependences of the Raman-shift line at $\sim 640 \text{ cm}^{-1}$ for PSMO and PSMFO samples. The Curie temperatures T_c and T_m for the two samples are indicated.

already become identifiable around ambient temperature (290 K), although $T_m = 95 \text{ K}$ and $T_c = 190 \text{ K}$ ($H = 5 \text{ kOe}$). The intensity at $T = 290 \text{ K}$ and below is much higher than that at $T = 300 \text{ K}$ and above. These findings clearly demonstrate the anomalous softening of the Mn–O bending and stretching modes well above T_c and T_m for this sample. In figure 5 the temperature of the line position for PSMFO is plotted too; this indicates the remarkable difference between the two samples. The line softening for PSMO initiates at $T \sim T_c$ with falling temperature, while for PSMFO the softening is observed well above T_c . We therefore conclude that there do indeed exist magnetic clusters in PSMFO well above T_c , whereas there are none in PSMO unless T is lowered to $T \sim 230 \text{ K}$, around T_c for PSMO.

Although the evidence provided by the Raman scattering is indirect as regards the magnetic ordering, it allows us to establish a qualitative correlation between the magnetic ordering and the transport behaviour for PSMO and PSMFO above their transition temperatures T_m . With the help of the data on the transport properties and magnetization measurement, we believe that the magnetic inhomogeneity in the Mn sites of PSMO caused by Fe doping does indeed contribute to the formation of magnetic clusters, and consequently to the magnetic polaron conduction. While it is believed that the increase of the ionic radius (r_A) of the La site caused by divalent-ion doping results in the softening of some vibration modes associated with the

Mn–O bond—for example, in the $\text{La}_{1-x}\text{Sr}_x\text{MnO}_3$ system [15, 16], we have not observed this effect in our PSMO system. However, what we suggest, for the first time, is that the Mn-site doping may cause the magnetic ordering phenomenon at a temperature above the Curie point T_c , at least for PSMFO.

In conclusion, we have presented an experimental investigation of the conduction mechanism of PSMFO ceramics ($\text{Fe} = 0.05$) above their Curie points, T_c . The Raman scattering data together with the transport properties and magnetization measurements allow us to conclude that the conduction of PSMFO is dominated by the magnetic polaron mechanism rather than the small-polaron mode. The magnetic ordering above the Curie point is attributed to the Mn-site inhomogeneity induced by Fe doping, which favours insulating behaviour and presents an antiferromagnetic background.

The authors would like to acknowledge the financial support from the Natural Science Foundation of China through the innovative group project and project 10074028 the National Key Project for Basic Research of China, CSMM of the National University of Singapore and the Laboratory of Laser Technologies of HUST.

References

- [1] Rao C N R and Raveau B 1998 *Colossal Magnetoresistance, Charge Ordering and Related Properties of Manganese Oxides* (Singapore: World Scientific)
- [2] Zener C 1951 *Phys. Rev.* **81** 440
- [3] Millis A J, Littlewood P B and Shraiman B I 1995 *Phys. Rev. Lett.* **74** 5144
- [4] Ziese M and Srinitiwara Wong C 1998 *Phys. Rev. B* **58** 11 519
- [5] Liu J-M, Huang Q, Li J, Ong C K, Wu Z C, Liu Z G and Du Y W 2000 *Phys. Rev. B* **62** 8976
- [6] Mott N 1993 *Conduction in Non-Crystalline Materials* (Oxford: Clarendon) p 17
- [7] Kusters R M, Singleton J, Keen D A, McGreevy R and Hayes W 1989 *Physica B* **155** 362
- [8] Lynn J W, Erwin R W, Borchers J A, Huang Q, Santoro A, Peng J L and Li Z Y 1996 *Phys. Rev. Lett.* **76** 4046
- [9] DeTeresa J M, Ibarra M R, Algarabel P A, Ritter C, Marquina C, Blasco J, Garcia J, Fermon C, Del Moral A and Arnold Z 1997 *Nature* **386** 256
- [10] Viret M, Glättli H, Fermon C, de Leon-Guevara A M and Revcolevschi A 1998 *Physica B* **241** 430
- [11] Chechersky V, Nath A, Isaac I, Franck J P, Ghosh K and Greene R L 2001 *Phys. Rev. B* **63** 052411
- [12] Ahn K H, Wu X W, Liu K and Chien C L 1996 *Phys. Rev. B* **54** 15 299
- [13] Righi L, Gorria P, Insausti M, Gutierrez J and Barandiaran J M 1997 *J. Appl. Phys.* **81** 5767
- [14] Huang Q, Li Z W, Li J and Ong C K 2001 *J. Appl. Phys.* **89** 7410
- [15] Pantoja A E, Trodahl H J, Buckley R G, Tomioka Y and Tokura Y 2001 *J. Phys.: Condens. Matter* **13** 3741 and references therein
- [16] Podobedov V B, Romero D B, Weber A, Rice J P, Shreekala R, Rajeswari M, Ramesh R, Venkatesan T and Drew H D 1998 *Appl. Phys. Lett.* **73** 3217